

# Dalton Transactions

An international journal of inorganic chemistry

Accepted Manuscript

This article can be cited before page numbers have been issued, to do this please use: N. Varnasari, F. Rouhani, A. Ramazani and A. Morsali, *Dalton Trans.*, 2020, DOI: 10.1039/D0DT00433B.



This is an Accepted Manuscript, which has been through the Royal Society of Chemistry peer review process and has been accepted for publication.

Accepted Manuscripts are published online shortly after acceptance, before technical editing, formatting and proof reading. Using this free service, authors can make their results available to the community, in citable form, before we publish the edited article. We will replace this Accepted Manuscript with the edited and formatted Advance Article as soon as it is available.

You can find more information about Accepted Manuscripts in the [Information for Authors](#).

Please note that technical editing may introduce minor changes to the text and/or graphics, which may alter content. The journal's standard [Terms & Conditions](#) and the [Ethical guidelines](#) still apply. In no event shall the Royal Society of Chemistry be held responsible for any errors or omissions in this Accepted Manuscript or any consequences arising from the use of any information it contains.

# Size and Function Influence Study on Enhanced Catalytic Performance of a Cooperative MOF for Mild, Green and Fast C-C Bond Formation

View Article Online

DOI: 10.1039/D0DT00433B

Najmeh Varnaseri<sup>†a</sup>, Farzaneh Rouhani<sup>†b</sup>, Ali Ramazani<sup>a, c\*</sup>, Ali Morsali<sup>b\*\*</sup>

<sup>a</sup> Department of Chemistry, Faculty of Sciences, University of Zanjan, P.O. Box 45195-313, Zanjan, Iran

<sup>b</sup> Department of Chemistry, Faculty of Sciences, Tarbiat Modares University, P.O. Box 14155-4838, Tehran, Iran

<sup>c</sup> Research Institute of Modern Biological Techniques (RIMBT), University of Zanjan, P.O. Box 10 45195-313, Zanjan, Iran

<sup>†</sup> Najmeh Varnaseri and Farzaneh Rouhani contributed equally to this work.

## Abstract

Tuning of pore function and size (surface area) are two key factors that play important roles in metal-organic-frameworks (MOFs) performance as catalyst. The catalytic performance of two bulk and nanosized MOFs with different functional groups such as Brønsted base and Lewis acid were studied in line with catalyst sustainable development and green chemistry principles. Bifunctional imine decorated TMU-33,  $[\text{Cd}_3(\text{BDC})_3(\text{OPP})(\text{DMF})_2].2\text{DMA}]_n$  (TMU-33), (OPP:N,N'-(oxybis(4,1-phenylene)) bis(1-(pyridin-4yl) methanimine)), with adjustable structure and amine functionalized TMU-40,  $[\text{Zn}(\text{BDC})(\text{L}^*)].\text{DMF}$ , ( $\text{L}^*$ : N<sub>1</sub>, N<sub>2</sub>-Bis (pyridin-4-ylmethylene) ethane-1,2-diamine) , were evaluated in the C-C bonding forming reaction in mild and green situation. The results show that nanosized samples of bifunctional TMU-33 which simultaneously have imine and open metal site, have higher performance as Knoevenagel catalyst. Furthermore, among nanosized samples, the nanoplate TMU-33 with more access to open metal sites shows the highest catalytic activity without any side product in water, room temperature at 5 min, that confirms the Lewis acid are

effective catalyst for this reaction. The catalyst could be reused for at least three cycles without significant loss of its activity. The performance of the structure indicates that tuning of functionality of MOFs can be very promising route for the extension of green catalysis.

**Key words:** Metal-Organic Framework (MOF), Catalyst, Knoevenagel Condensation, Green Solvent, Mild Situation

## 1. Introduction

The growing population has a crucial requirement for the production of fine chemicals. The development of more efficient, selective and versatile catalysts can be the key to resolve the demand<sup>1</sup>. Metal-organic frameworks (MOFs) have been noticed because of tunable porosity, design ability, uniform and accessible catalytic centers and chemical and thermal stability<sup>2-5</sup>. Therefore, they can be tunable and suitable catalysts for most of the organic reactions. Some reactions have been catalyzed by MOFs as solid acid catalysts or catalyst supports such as Knoevenagel condensation, trans esterification, aldol condensation, oxidation, epoxide ring-opening reaction and so on<sup>6-19</sup>.

The Knoevenagel condensation of carbonyl groups (aldehyde and ketone) with active methylene species is one of the methods to form C=C bonds, and it has numerous applications in industrial organic synthesis<sup>20</sup>. In literature, the reaction of aldehydes and their derivatives, are reported frequently because the reaction of ketones with malononitrile need to harsher conditions<sup>21</sup>. The Knoevenagel reaction has been reported by both basic<sup>22</sup> and acidic<sup>23</sup> catalysts but activity of the acidic catalysts is lower<sup>24</sup>. On the other hand, the polarity of solvent has a remarkable effect on performance of MOFs as Knoevenagel reaction catalyst<sup>25</sup>. Polar solvents actually stabilize the charged transition-state intermediate of the Knoevenagel condensation<sup>26</sup>. A large diversity of homogeneous and heterogeneous catalysts are applied to this reaction and they show different features<sup>27-28</sup>. Heterogeneous catalysis offer several advantages over homogeneous ones<sup>29</sup>, because they have more recyclability,

reusability easier separation and they minimized the undesired waste<sup>30</sup>. MOFs can serve as heterogeneous catalysts either by the metal ion or cluster as Lewis acid or functional ligands as active sites that incorporated through direct synthesis or by post-synthetic modification<sup>31</sup>. There has been enormous investigations on the catalytic performance of catalysis taking place at the metal center<sup>32-33</sup>. However, only few studies have been reported on MOFs with catalytically-active functional organic sites<sup>34</sup>. This is because, the functional groups need to be free and accessible to the substrates and cannot be directly connected to the metal ions of the MOF<sup>35-36</sup>. The numbers of heterogeneous catalysts including MOFs with various kinds of basic sites have been offered to catalyze Knoevenagel condensation<sup>37-38</sup>. Several possible mechanisms have been proposed for the reaction according to the catalysts structure<sup>39-40</sup>. For catalysts with high base strength, the active methylene reactant is deprotonated by basic sites and carbanion formed. The addition-elimination process is facilitated which occurs between carbanion and the carbonyl carbon atom of aldehyde. For weaker bases such as MOFs carrying amino groups at their structures, it has been proposed that the reaction occurs between the surface amine sites and aldehyde molecule to form an imine intermediate and one molecule of water<sup>21</sup>. Final product is yielded and regenerate the amine catalyst by a molecular arrangement in methylene<sup>41-42</sup>. The Knoevenagel condensation has usually been considered as a classical test reaction to evaluate the basicity of catalysts<sup>43</sup>.

Although various catalytic systems have been reported to date, development of catalyst which can promote this reaction without the formation of side products is still a challenge. In addition to formation of side products, a reaction between the solvent and the aldehyde is possible<sup>44</sup>. From a general point of view, the development of catalyst systems in non-toxic solvent, at mild condition, methodology without environmental concern is very useful in the field of green chemistry. In order to design the high effective catalyst, we used the TMU-33, nanosized samples of TMU-33 and TMU-40 as catalyst. The TMU-33 framework has an

open metal site and an imine functional group that can both act as catalysts separately or simultaneously<sup>45</sup>. Also, the structure of TMU-40 has active amines available for catalytic reaction<sup>46</sup>. The results indicate that nanosized TMU-33 is a more effective catalyst due to the simultaneous acid-base part of the (TMU-33) structure. Based on the results, the nanoplate structure of TMU-33 with more abundant of the open metal site demonstrate the best catalytic species for this reaction.

## 2. Experimental

### 2.1. Material and method

All chemicals without any purification were obtained from Sigma-Aldrich and Merck companies. The progress of the catalytic reactions was monitored by an Echrom GC A90 gas chromatograph. Synthesis methods of N,N'-(oxybis(4,1-phenylene))bis(1-(pyridin-4-yl)methanimine) (OPP) and N<sub>1</sub>, N<sub>2</sub>-bis (pyridin-4-ylmethylene) ethane-1,2-diamine(L) ligand expressed in S.I.

### 2.2. Synthesis of [Cd<sub>3</sub>(BDC)<sub>3</sub>(OPA)(DMF)<sub>2</sub>].2DMA (TMU-33)

TMU-33 was synthesized using the previously-reported method<sup>45</sup>. The mixture of Cd(NO<sub>3</sub>)<sub>2</sub>·4H<sub>2</sub>O (1 mmol, 0.3048 g), OPP (1 mmol, 0.378 g) and terephthalic acid (H<sub>2</sub>BDC) (1 mmol, 0.0188 g) added to 20mL DMF solvent and subjected to solvothermal reaction conditions in glass vials for 72 h at 80°C. The generated precipitate was separated by filtration, washed repeatedly with DMF and air-dried. Before the catalysis process, for removing guest DMF molecules, the resulting precipitate was dispersed in acetonitrile for 72 h and the solvent exchanged three times. The solution was vacuum filtered and the solid was dried in oven at 80 °C.

### 2.3. Synthesizes of [Cd(BDC)(L\*)]. DMF (TMU-40)

L(1mmol,0.256 g), H<sub>2</sub>BDC (1mmol, 0.166 g) and Cd(NO<sub>3</sub>)<sub>2</sub>·4H<sub>2</sub>O (1 mmol, 0.3048 g), and 20 ml DMF was mixed and then heated to 120 °C for 72 h to form dark red crystals of TMU-

40 <sup>46</sup>. After crystal formation, they washed with ethanol and dried. For obtaining active TMU-40, the crystals were immersed in dichloromethane for 24 h and the solvent exchanged every 12h. Solvent was decanted and the powder dried in oven at 80 °C.

#### 2.4. Synthesis of TMU-33 Nanostructures

TMU-33 nanostructures synthesize via sonochemical reaction in ultrasonic bath. TMU-33 nanostructures were synthesized by a concentrations of  $[H_2BDC] = [Cd(OAc)_2 \cdot 4H_2O] = [OPP \text{ ligand}]$  of [0.001] and optimal concentrations of benzoic acid and pyridine as capping reagents (modulator), respectively at room temperature for 20 min. These capping agents are chosen due to similarity of their coordination sites to  $H_2BDC$  and OPP ligand, respectively. The "r" factor is ratio of [capping reagent]/ [OPP], for nanorod TMU-33, "r" factor is defined as the ratio [benzoic acid]/  $[H_2BDC]$  were 10, 5 and 2, and r factors for [pyridine]/ [OPP ligand] about nanoplates also were 10, 5 and 2. The solid was washed with DMF then filtered under vacuum and dried in oven at 100°C <sup>45</sup>.

#### 2.5. Catalytic experiments

The catalytic reactions were carried out following green conditions, with 1 mg of catalysts at room temperature using water as solvent. In a typical catalytic experiment, aromatic aldehyde with different structure (0.1mmol) and malononitrile (0.25mmol) in 3 ml water was stirred at room temperature for 5 min with 1 mg of the activated catalysts. The reaction was monitored by gas chromatography until completion of the reaction.

### 3. Results and discussion

TMU-40 (CCDC number: 1811813) was synthesized by the reaction of 1,2- $N_1, N_2$ -bis(pyridin-4-ylmethylene)ethane (ligand L)  $Cd(NO_3)_2 \cdot 6H_2O$  and  $H_2BDC$  in DMF at 120°C for 72 h. The ligand  $L^* = 5,6$ -dipyridin-4-yl-1,2,3,4-tetrahydropyrazine synthesized through an in-situ C=C formation. Such aldimine C=C coupling reactions catalyzed by cyanide ion

reported previously by Strain in 1824<sup>47-48</sup>. The steps of L\* formation are schematically illustrated in **Figure 1** and the proposed mechanism are presented as **Figure S1**.

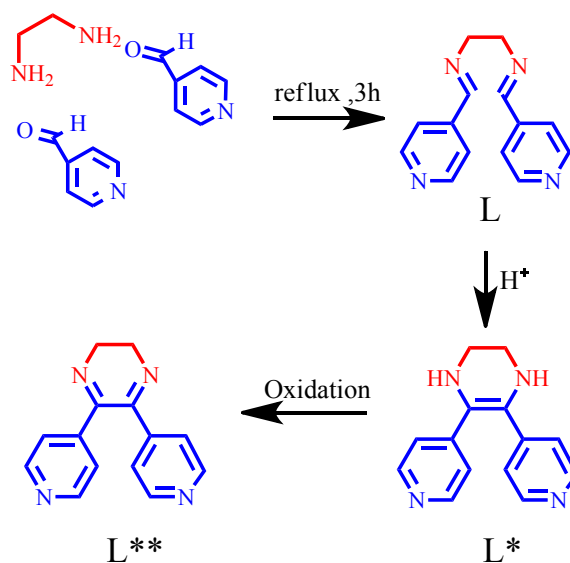


**Figure 1.** Synthesis route of L and C=C coupling reaction of L to L\*\*.

The 3D framework of the TMU-40(Cd) with expecting 4-connected sql tetragonal plane net crystallizes in the orthorhombic space group  $P_{bca}$ . The structure of  $[Cd(H_2BDC)(L^*)].DMF$  extended in three dimensions through hydrogen bonding. Pore sizes evaluated from single-crystal X-ray structure is  $5.5 \times 7.9 \text{ \AA}$  and has  $13 \text{ \AA}^3$  free voids (**Figure 2A**). The thermogravimetric analysis (TGA) has been carried out on TMU-40 in the range of 25–600 °C. The thermogravimetric curve of TMU-40(Cd) shows a weight loss of 13.1% at about 200 °C, corresponding to removal of trapped solvent in the pores. As can be seen in **Figure 2B**, the structure is stable at temperatures up to 360 °C.

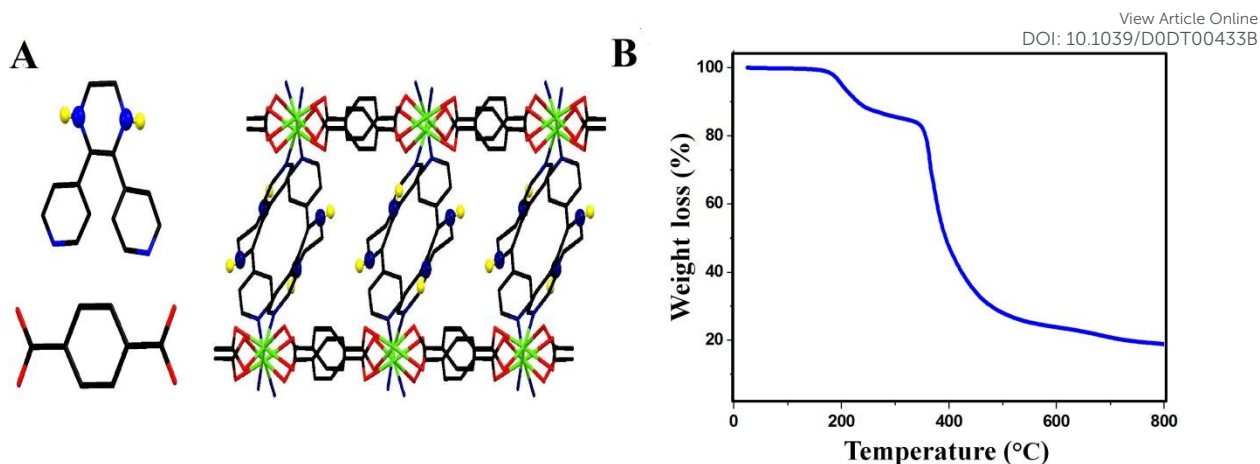


**Figure 2.** (A) The schematic pictures of constructive part and 3D expansion of TMU-40, (B) Thermogravimetric analysis of TMU-40. Color code: C: black; O: red; N: blue, Cd: green and H: yellow.

On the other hand, solvothermal reaction of  $\text{Cd}(\text{NO}_3)_2 \cdot 4\text{H}_2\text{O}$ , V-shaped imine based ligand (OPP) and  $\text{H}_2\text{BDC}$  in DMF at  $100^\circ\text{C}$  for 72 h afforded a MOF by the following framework formula:  $[\text{Cd}_3 (\text{BDC})_3 (\text{OPA}) (\text{DMF})_2] \cdot 2\text{DMA}$  (TMU-33) (CCDC number: 1522499). The imine based ligand OPP was readily synthesized by a nucleophilic substitution reaction of 4,4'-oxydianiline and 4-pyridine carboxaldehyde in good yield and gram scale. The OPP is a typical flexible ligand with rotating around a single bond (one  $\text{sp}^3$  hybrid atom on its backbones) linking to a quaternary carbon atom. In particular, 4 BDC<sup>2-</sup> anions are in the bridging mode and two others have two-coordination position. More crystallography data are presented in our previous paper<sup>45</sup>. The 3D framework of TMU-33 with rectangle channels ( $6.6 \times 6.4 \text{ \AA}$ ) along the b axis contains of two non-coordinated DMA molecules which are formed by partial hydrolysis of solvent (DMF) during synthesis procedures. The activation process was done by immersion of obtained samples in  $\text{CH}_3\text{CN}$  for 72h. The fresh solvent was added every 12 h. The double interpenetration of TMU-33 with formed  $6.6 \times 6.4 \text{ \AA}$  rectangular pores is presented in **Figure 3A**. The TGA results shown in **Figure 3D** also illustrate the loss of two free dimethylamine (DMA) molecules and two coordinated DMF

molecules in the temperature range of 25-260°C. Further increase of temperature led to loss of the coordinated OPP ligand and the disintegration of the framework at about 300. The TG analyses of TMU-33 crystal, as synthesized sample in green, TMU-33 after coordinated DMF removal in black and after DMA in red are shown in **Figure 3D**.

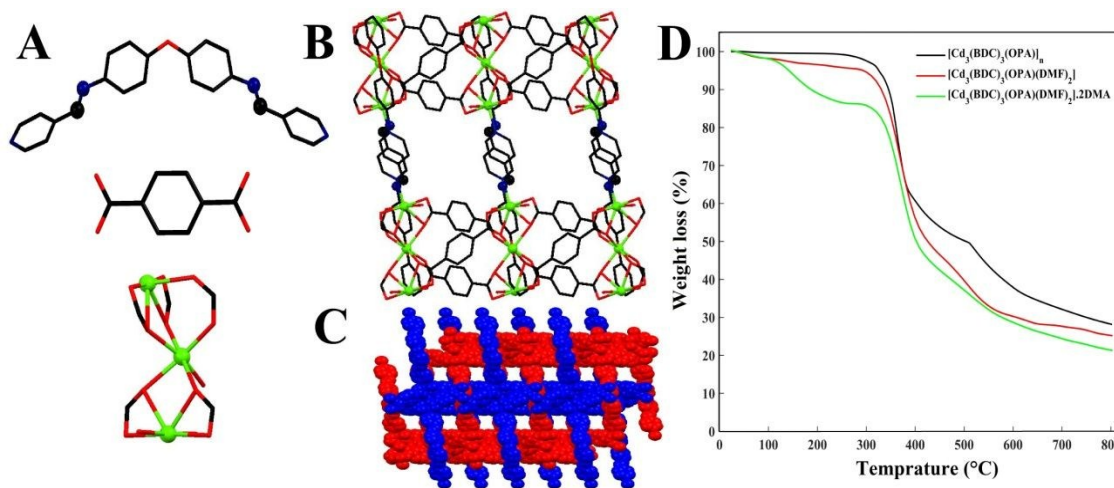


**Figure 3.** (A) Schematic picture of OPP, H<sub>2</sub>BDC and Cd<sub>3</sub> SBU, (B) 3D expansion and (C) two fold interpenetration TMU-33, (D) Thermogravimetric analyses of TMU-33 (green), TMU-33 after DMF removal (black) after removal DMA (red). Color code: C: black; O: red; N: blue, Cd: green and H: yellow.

Nanoplate and nanorods samples of TMU-33 were synthesized in ultrasonic bath by using pyridine and benzoic acid as capping reagents, respectively. These capping agents are chosen due to similarity of their coordination sites to H<sub>2</sub>BDC and OPP ligand, respectively. The "r" factor is ratio of [capping reagent]/ [OPP], where benzoic acid and pyridine are capping reagent in nanorod and nanoplate morphology, respectively.

For the study of the effect of concentration of the initial reagents on size and morphology of nano-structured TMU-33, the above processes were performed with concentrations of [BDC] = [Cd(OAc)<sub>2</sub>·4H<sub>2</sub>O] = [OPA ligand] of [0.05], [0.01] and [0.005] M. For TMU-33 nanorods and nanoplates, the above processes were performed with concentrations of [BDC] = [Cd(OAc)<sub>2</sub>·4H<sub>2</sub>O] = [OPA ligand] of [0.05] by adding different concentrations of benzoic acid and pyridine as capping reagents (modulator) at ambient for 20 min. The resulting powder was isolated by centrifugation, washed with DMF three times and dried in air for

characterization. The morphology of the MOF samples was determined by SEM (Figure 4). View Article Online  
DOI: 10.1039/C9DT00433B

Apparently, the morphologies and dimensions of the product are strongly dependent on the reaction conditions. It is found that the sonication time, concentration of starting reagents and sonication power plays the dominating roles in the final morphology of product (in order to control of nucleation). As a result, for the preparation of optimal nanorod and nanoplate samples, concentration of [0.001] M of each reactant, 20 minutes for sonication time and 24W as sonication power using as synthesis conditions.

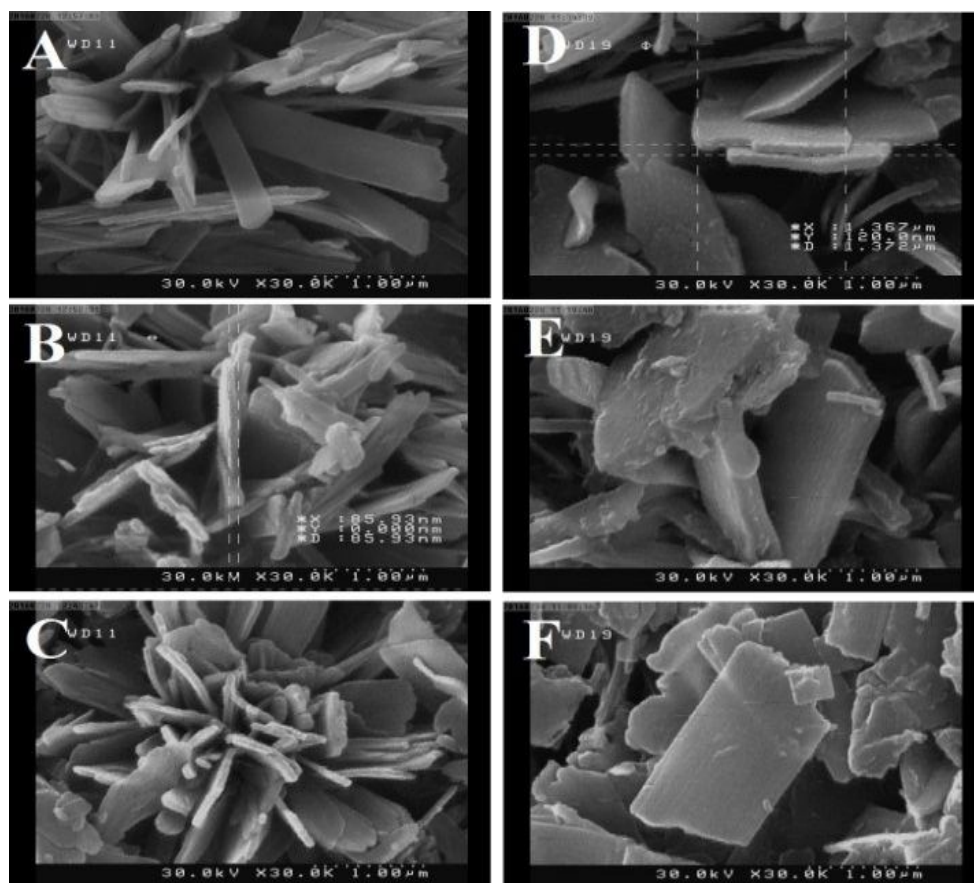


**Figure 4.** SEM images of nanorod morphology with  $r=2$  (A),  $r=5$  (B) and  $r=10$  (C) of TMU-33, and nanoplate morphology with  $r=2$  (D),  $r=5$  (E) and  $r=10$  (F) of TMU-33.

Powder X-ray diffraction (XRD) measurements demonstrate that nano-sized samples of TMU-33 were structurally similar to TMU-33 prepared via solvothermal (Figure S2). A homogeneous distribution of active sites, microenvironments, transmission channels and the

presence of functional groups on the inner surface of the MOF voids and channels lead to the distinct catalytic properties of MOF catalysts<sup>49</sup>. It is clear that accessibility of both metal nodes and functionality of ligands make MOFs great candidates for application in catalytic area. To select the best condensation reaction catalyst, we divided our studies into three sections. We first used the crystalline structure of TMU-33 which has the open metal site and imine vacancy and TMU-33 which has an amine as the catalytic site.

To examine the catalytic activity of the TMU-33 and TMU-40 frameworks which have different size and function groups (amine, imine and open metal site), the Knoevenagel condensation as a base-catalyzed model reaction was carried out. 0.1 mmol benzaldehyde, 0.25 mmol malononitrile and 1mg catalyst were added into a glass reactor with 3 ml of different solvents at room temperature. A range of solvents were employed to optimize the reaction solvent leading to increase the yield. The higher yields of target products were obtained in polar protic solvents (Table 1). However, the reaction under solvent-free conditions was slow. Therefore, water was selected as reaction solvent.

**Table 1.** Control reactions for finding the optimal condensation for TMU-33 and TMU-40 as Knoevenagel condensation reaction with 4-chlorobenzaldehyde and malononitrile.

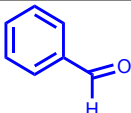
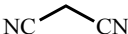
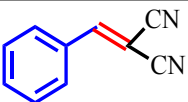
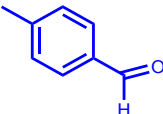
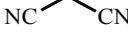
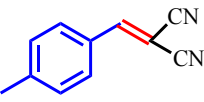
Entry	Catalyst	Amount of catalyst	Solvent	Temperature(°C)	Time (min)	Yield (%)
1	TMU-33	1 mg	H <sub>2</sub> O	r.t	5	99
2	TMU-33	1 mg	EtOH	r.t	5	28
3	TMU-33	1 mg	MeOH	r.t	5	24
4	TMU-33	1 mg	CH <sub>3</sub> CN	r.t	5	11
5	TMU-33	1 mg	Toluene	r.t	5	4
6	TMU-40	1 mg	H <sub>2</sub> O	r.t	5	92
7	TMU-40	1 mg	EtOH	r.t	5	21
8	TMU-40	1 mg	MeOH	r.t	5	27
9	TMU-40	1 mg	CH <sub>3</sub> CN	r.t	5	9
10	TMU-40	1 mg	Toluene	r.t	5	4
11	---	---	H <sub>2</sub> O	r.t	5	17
12	---	---	EtOH	r.t	5	10
13	---	---	MeOH	r.t	5	14
14	---	---	CH <sub>3</sub> CN	r.t	5	2

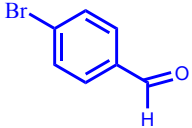
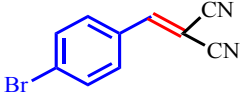
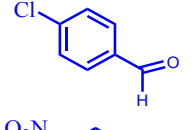
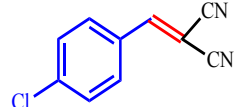
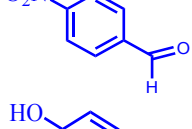
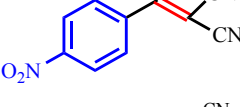
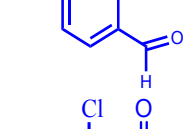
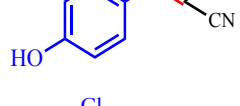
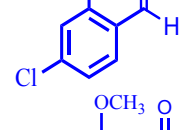
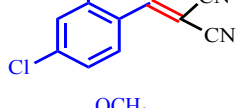
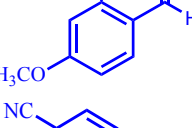
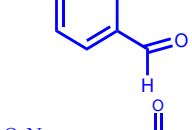
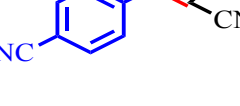
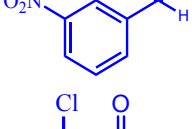
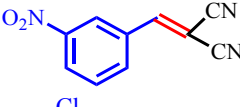
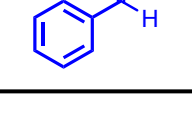
15	---	---	Toluene	r.t	5	90
16	TMU-33	0.5 mg	H <sub>2</sub> O	r.t	5	75
17	TMU-33	2 mg	H <sub>2</sub> O	r.t	5	99
18	TMU-33	1 mg	H <sub>2</sub> O	35	>5	99
19	TMU-33	1 mg	H <sub>2</sub> O	45	2	99

View Article Online  
DOI: 10.1039/D0DT00433B

To probe the optimal amount of catalyst, a solution of 4-chlorobenzaldehyde (0.1mmol) and malononitrile (0.25 mmol) was loaded into two glass vessels. Then 1 mg of catalysts were added to each one and allowed to react with active methylene compounds. The stirring continued at room temperature and progress of the reaction is monitored by GC. Also, different amount of catalyst and higher temperature were studied. The catalytic results indicate the reactions could be done on 1 mg of the catalysts at room temperature in 3 ml of H<sub>2</sub>O and one product was obtained in the best yield (**Table 1**). Survey of results reveals that one product is formed and no by-products were observed in our analyses. As shown in **Table 2**, we investigated aldehydes with different substituents as substrates to compare the catalytic activity of the MOFs. The structure and purity of the products were analyzed using <sup>1</sup>H NMR spectroscopy (Figure S3-S11). Reactions progress was monitored by GC (Figure S12-S22). About all of the reagents, the catalytic performance of TMU-33 is better than that of TMU-40 which could be attributed to better functionality of open metal site or imine as catalyst.

**Table 2.** Knoevenagel condensation reaction catalyzed by TMU-33 and TMU-40 in the presence of various aldehydes (reaction conditions: substrates (0.1mmol), malononitrile (0.25mmol), 1mg catalyst, solvent: H<sub>2</sub>O (3ml), r.t., 5 min)

Entry	Catalyst	Substrate	Substrate	Product	Yield (%)
1	TMU-33				74
	TMU-40				61
2	TMU-33				58
	TMU-40				67

3	TMU-33 TMU-40				88 79	View Article Online DOI: 10.1039/D0DT00433B
4	TMU-33 TMU-40				98 92	
5	TMU-33 TMU-40				92 90	
6	TMU-33 TMU-40				85 73	
7	TMU-33 TMU-40				75 63	
8	TMU-33 TMU-40				79 71	
9	TMU-33 TMU-40				94 90	
10	TMU-33 TMU-40				82 80	
11	TMU-33 TMU-40				68 56	

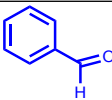
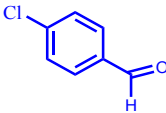
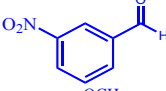
In the second part of study, to evaluate the size effect, nanosized samples of TMU-33 with different morphologies were used as catalyst. In nanoplate sample, the relative accessibility of Lewis acid on the external surface of the catalyst is more than that of Brønsted base. On the other hand, in nanorod sample, there is more relative accessibility to Brønsted base (Table 3).

**Table 3.** The catalytic sites in different catalysts.

Entry	Catalyst	Active site
1	TMU-40	amine group
2	TMU-33	imine group + open metal site
3	Nanorod TMU-33	imine group more accessible than open metal site

The presented results in **Table 4** demonstrate that the nanostructures are more effective catalyst due to the higher accessibility of catalytic sites in compare of bulk structure. Furthermore, the catalytic performance of the nanoplate sample is better than that of the other samples regardless electron donating or electron withdrawing groups of the aldehyde. This indicates that the nanoplate-TMU-33 catalyst is a high performance catalyst in Knoevenagel condensation reaction.

**Table 4.** Knoevenagel condensation reaction catalyzed by bulk and nanosized TMU-30.

Entry	Substrate	Catalyst	Yield (%)
1		TMU-33	74
		Nanorod TMU-33	96
		NanoplateTMU-33	100
2		TMU-33	98
		Nanorod TMU-33	95
		NanoplateTMU-33	99
3		TMU-33	92
		Nanorod TMU-33	92
		NanoplateTMU-33	96
4		TMU-33	79
		Nanorod TMU-33	89
		NanoplateTMU-33	90
5		TMU-33	75
		Nanorod TMU-33	92
		NanoplateTMU-33	92

In order to investigate the reusability of TMU-33 and TMU-40, the catalyst was separated from the reaction product by centrifugation. The PXRD patterns of catalysts studied after 3 run reactions. The intact patterns show that the recycled catalyst can be reused at least 3 runs without any loss of intrinsic catalytic activity (Figure S23). A comparison of the catalytic

activity of nanostructure TMU-33 and TMU-33 with that of other heterogeneous catalysts previously used in Knoevenagel condensation reaction is reported in **Table 5**.

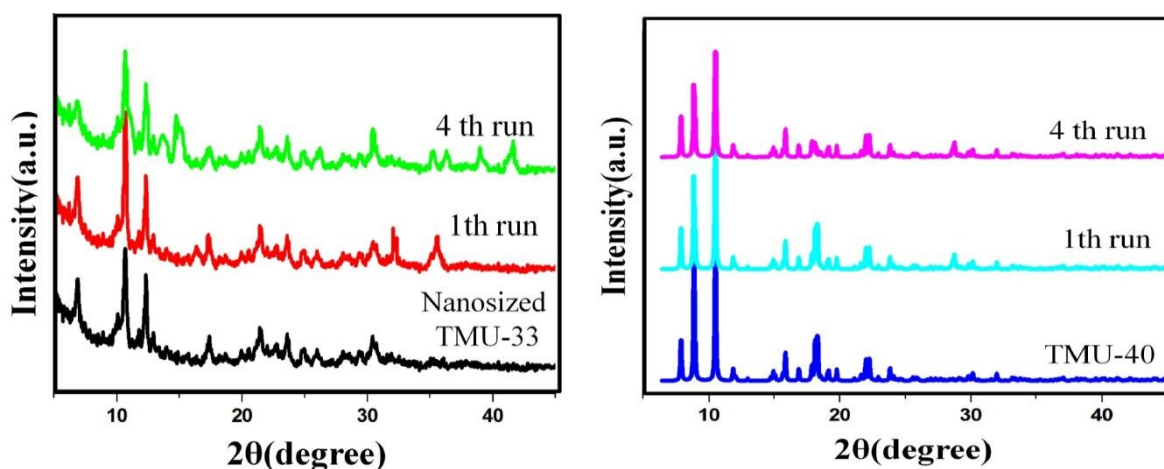


**Figure 5.** PXRD of nanostructure TMU-33 (left) and TMU-40 (right) recovered after the first and fourth catalytic cycles.

**Table 5.** Knoevenagel condensation reactions of benzaldehyde and malononitrile catalyzed by different catalysts.

Entry	Catalyst	Amount	Time	Solvent	Temp [°C]	Yield	Ref
1	$\{[\text{Ni}_3(\text{TBIB})_2(\text{BTC})_2(\text{H}_2\text{O})_6] \cdot 5\text{C}_2\text{H}_5\text{O} \cdot 9\text{H}_2\text{O}\}_n$	5 mol%	2h	DCM	60	100	49
2	Au@Cu(II)-MOF(1)	3 mol%	23h	Toluene/MeOH	r.t.	99	50
3	ZIF-9	5 mol%	4h	Toluene	r.t.	99	51
4	$\{[\text{Zn}(\text{Py}_2\text{TTz})(2\text{-NH}_2\text{BDC})] \cdot (\text{DMF})_n\}$	2mol%	6h	Free solvent	60	99.9	52
5	$[\text{Gd}_2(\text{tnbd})_3(\text{DMF})_4] \cdot 4\text{DMF} \cdot 3\text{H}_2\text{O}$	10 mol%	20 min	$\text{C}_6\text{H}_6$	r.t.	96	53
6	CAU-1-NH <sub>2</sub>	25 mg	7h	EtOH	40	100	44
7	NH <sub>2</sub> (50%)-MIL-53	5.3 mg/mL	5h	MeOH	80	100	54
8	Schiff base supported MCM-41	5mg	6h	H <sub>2</sub> O	r.t.	99	55
9	Nanoplate TMU-33	10mg	5min	H <sub>2</sub> O	r.t.	100	This work

#### 4. Conclusion

The catalytic performance of four bulk and nanosized MOFs with different functionality such as Brønsted base and Lewis acid and different frequencies of functional group studied for Knoevenagel reaction. By nanosized TMU-33 as catalyst, the conversion easily reached more

than 90% under mild condition with a low amount of catalyst and the short time. Between four used catalysts, nanoplate sample in which the relative accessibility of open metal site on the external surface of the catalyst is more than that of Brønsted base is better than the other samples regardless electron donating or electron withdrawing groups of the aldehyde. The results show that open metal site as Lewis acid is better catalyst for Knoevenagel condensation. Indeed this study highlights the important role of size and accessibility of catalytic site in the catalytic performance.

### Conflicts of interest

There are no conflicts to declare.

### Acknowledgments

This work was supported by the “Iran National Science Foundation: INSF”, “Tarbiat Modares University” and “University of Zanjan”.

### References

1. Položij, M.; Rubeš, M.; Čejka, J.; Nachtigall, P., Catalysis by Dynamically Formed Defects in a Metal–Organic Framework Structure: Knoevenagel Reaction Catalyzed by Copper Benzene-1, 3, 5-tricarboxylate. *ChemCatChem* **2014**, *6* (10), 2821-2824.
2. Ranocchiari, M.; van Bokhoven, J. A., Catalysis by metal–organic frameworks: fundamentals and opportunities. *Physical Chemistry Chemical Physics* **2011**, *13* (14), 6388-6396.
3. Rouhani, F.; Gharib, B.; Morsali, A., Solvent switching smart metal–organic framework as a catalyst of reduction and condensation. *Inorganic Chemistry Frontiers* **2019**, *6* (9), 2412-2422.
4. Rouhani, F.; Morsali, A.; Retailleau, P., Simple One-Pot Preparation of a Rapid Response AIE Fluorescent Metal–Organic Framework. *ACS applied materials & interfaces* **2018**, *10* (42), 36259-36266.
5. Das, A.; Anbu, N.; Mostakim, S.; Dhakshinamoorthy, A.; Biswas, S., A functionalized UiO-66 MOF for turn-on fluorescence sensing of superoxide in water and efficient catalysis for Knoevenagel condensation. *Dalton Transactions* **2019**, *48* (46), 17371-17380.
6. Chen, J.; Liu, R.; Gao, H.; Chen, L.; Ye, D., Amine-functionalized metal-organic frameworks for the transesterification of triglycerides. *Journal of Materials Chemistry A* **2014**, *2* (20), 7205-7213.
7. Saha, D.; Sen, R.; Maity, T.; Koner, S., Porous magnesium carboxylate framework: Synthesis, X-ray crystal structure, gas adsorption property and heterogeneous catalytic aldol condensation reaction. *Dalton Transactions* **2012**, *41* (24), 7399-7408.

8. i Xamena, F. L.; Casanova, O.; Tailleux, R. G.; Garcia, H.; Corma, A., Metal organic frameworks (MOFs) as catalysts: A combination of Cu<sup>2+</sup> and Co<sup>2+</sup> MOFs as an efficient catalyst for tetralin oxidation. *Journal of Catalysis* **2008**, *255* (2), 220-227. View Article Online  
DOI: 10.1039/D0DT00433B
9. Liu, Y.; Klet, R. C.; Hupp, J. T.; Farha, O., Probing the correlations between the defects in metal–organic frameworks and their catalytic activity by an epoxide ring-opening reaction. *Chemical Communications* **2016**, *52* (50), 7806-7809.
10. Song, F.; Wang, C.; Falkowski, J. M.; Ma, L.; Lin, W., Isoreticular chiral metal– organic frameworks for asymmetric alkene epoxidation: tuning catalytic activity by controlling framework catenation and varying open channel sizes. *Journal of the American Chemical Society* **2010**, *132* (43), 15390-15398.
11. Horike, S.; Dinca, M.; Tamaki, K.; Long, J. R., Size-selective Lewis acid catalysis in a microporous metal-organic framework with exposed Mn<sup>2+</sup> coordination sites. *Journal of the American Chemical Society* **2008**, *130* (18), 5854-5855.
12. Pan, L.; Liu, H.; Lei, X.; Huang, X.; Olson, D. H.; Turro, N. J.; Li, J., R<sub>2</sub>PM-1: A recyclable nanoporous material suitable for ship-in-bottle synthesis and large hydrocarbon sorption. *Angewandte Chemie International Edition* **2003**, *42* (5), 542-546.
13. Zhang, F.; Shi, J.; Jin, Y.; Fu, Y.; Zhong, Y.; Zhu, W., Facile synthesis of MIL-100 (Fe) under HF-free conditions and its application in the acetalization of aldehydes with diols. *Chemical Engineering Journal* **2015**, *259*, 183-190.
14. Wu, C.-D.; Hu, A.; Zhang, L.; Lin, W., A homochiral porous metal– organic framework for highly enantioselective heterogeneous asymmetric catalysis. *Journal of the American Chemical Society* **2005**, *127* (25), 8940-8941.
15. Hu, A.; Ngo, H. L.; Lin, W., Chiral, porous, hybrid solids for highly enantioselective heterogeneous asymmetric hydrogenation of β-keto esters. *Angewandte Chemie International Edition* **2003**, *42* (48), 6000-6003.
16. Hu, A.; Ngo, H. L.; Lin, W., Chiral porous hybrid solids for practical heterogeneous asymmetric hydrogenation of aromatic ketones. *Journal of the American Chemical Society* **2003**, *125* (38), 11490-11491.
17. Oozeerally, R.; Burnett, D. L.; Chamberlain, T. W.; Walton, R. I.; Degirmenci, V., Exceptionally Efficient and Recyclable Heterogeneous Metal–Organic Framework Catalyst for Glucose Isomerization in Water. *ChemCatChem* **2018**, *10* (4), 706-709.
18. Tanaka, K.; Sakuragi, K.; Ozaki, H.; Takada, Y., Highly enantioselective Friedel–Crafts alkylation of N, N-dialkylanilines with trans-β-nitrostyrene catalyzed by a homochiral metal–organic framework. *Chemical communications* **2018**, *54* (49), 6328-6331.
19. Agarwal, R. A.; Mukherjee, S., Two-dimensional flexible Ni (II)-based porous coordination polymer showing single-crystal to single-crystal transformation, selective gas adsorption and catalytic properties. *Polyhedron* **2016**, *105*, 228-237.
20. Lee, A.; Michrowska, A.; Sulzer-Mosse, S.; List, B., The catalytic asymmetric Knoevenagel condensation. *Angewandte Chemie International Edition* **2011**, *50* (7), 1707-1710.
21. Zhang, Y.; Wang, Y.; Liu, L.; Wei, N.; Gao, M.-L.; Zhao, D.; Han, Z.-B., Robust bifunctional lanthanide cluster based metal–organic frameworks (MOFs) for tandem Deacetalization–Knoevenagel reaction. *Inorganic chemistry* **2018**, *57* (4), 2193-2198.
22. Smith, M. B.; March, J., *March's advanced organic chemistry: reactions, mechanisms, and structure*. John Wiley & Sons: 2007.
23. Hu, Z.; Zhao, D., Metal–organic frameworks with Lewis acidity: synthesis, characterization, and catalytic applications. *CrystEngComm* **2017**, *19* (29), 4066-4081.

24. Saravanamurugan, S.; Palanichamy, M.; Hartmann, M.; Murugesan, V., Knoevenagel condensation over  $\beta$  and Y zeolites in liquid phase under solvent free conditions. *Applied Catalysis A: General* **2006**, *298*, 8-15. View Article Online  
DOI: 10.1039/B5DT00433B
25. Yang, Y.; Yao, H.-F.; Xi, F.-G.; Gao, E.-Q., Amino-functionalized Zr (IV) metal–organic framework as bifunctional acid–base catalyst for Knoevenagel condensation. *Journal of Molecular Catalysis A: Chemical* **2014**, *390*, 198-205.
26. Rodriguez, I.; Sastre, G.; Corma, A.; Iborra, S., Catalytic activity of proton sponge: Application to Knoevenagel condensation reactions. *Journal of Catalysis* **1999**, *183* (1), 14-23.
27. Zhu, A.; Liu, R.; Li, L.; Li, L.; Wang, L.; Wang, J., Dual functions of N, N-dimethylethanolammonium-based ionic liquids for the Knoevenagel reactions at room temperature. *Catalysis today* **2013**, *200*, 17-23.
28. Luan, Y.; Qi, Y.; Gao, H.; Andriamitantoa, R. S.; Zheng, N.; Wang, G., A general post-synthetic modification approach of amino-tagged metal–organic frameworks to access efficient catalysts for the Knoevenagel condensation reaction. *Journal of Materials Chemistry A* **2015**, *3* (33), 17320-17331.
29. Liu, L.; Corma, A., Metal catalysts for heterogeneous catalysis: from single atoms to nanoclusters and nanoparticles. *Chemical reviews* **2018**, *118* (10), 4981-5079.
30. Lee, J.; Farha, O. K.; Roberts, J.; Scheidt, K. A.; Nguyen, S. T.; Hupp, J. T., Metal–organic framework materials as catalysts. *Chemical Society Reviews* **2009**, *38* (5), 1450-1459.
31. Vermoortele, F.; Bueken, B.; Le Bars, G. I.; Van de Voorde, B.; Vandichel, M.; Houthoofd, K.; Vimont, A.; Daturi, M.; Waroquier, M.; Van Speybroeck, V., Synthesis modulation as a tool to increase the catalytic activity of metal–organic frameworks: the unique case of UiO-66 (Zr). *Journal of the American Chemical Society* **2013**, *135* (31), 11465-11468.
32. Pérez-Mayoral, E.; Musilová, Z.; Gil, B.; Marszalek, B.; Položij, M.; Nachtigall, P.; Čejka, J., Synthesis of quinolines via Friedländer reaction catalyzed by CuBTC metal–organic-framework. *Dalton Transactions* **2012**, *41* (14), 4036-4044.
33. Tonigold, M.; Lu, Y.; Bredenkötter, B.; Rieger, B.; Bahn Müller, S.; Hitzbleck, J.; Langstein, G.; Volkmer, D., Heterogeneous Catalytic Oxidation by MFU-1: A Cobalt (II)-Containing Metal–Organic Framework. *Angewandte Chemie International Edition* **2009**, *48* (41), 7546-7550.
34. Dhakshinamoorthy, A.; Garcia, H., Metal–organic frameworks as solid catalysts for the synthesis of nitrogen-containing heterocycles. *Chemical Society Reviews* **2014**, *43* (16), 5750-5765.
35. Corma, A.; García, H.; Llabrés i Xamena, F., Engineering metal organic frameworks for heterogeneous catalysis. *Chemical reviews* **2010**, *110* (8), 4606-4655.
36. Yoon, M.; Srirambalaji, R.; Kim, K., Homochiral metal–organic frameworks for asymmetric heterogeneous catalysis. *Chemical reviews* **2011**, *112* (2), 1196-1231.
37. Liu, J.; Chen, L.; Cui, H.; Zhang, J.; Zhang, L.; Su, C.-Y., Applications of metal–organic frameworks in heterogeneous supramolecular catalysis. *Chemical Society Reviews* **2014**, *43* (16), 6011-6061.
38. Gao, M.-L.; Qi, M.-H.; Liu, L.; Han, Z.-B., An exceptionally stable core–shell MOF/COF bifunctional catalyst for a highly efficient cascade deacetalization–Knoevenagel condensation reaction. *Chemical Communications* **2019**, *55* (45), 6377-6380.
39. Su, F.; Antonietti, M.; Wang, X., mpg-C 3 N 4 as a solid base catalyst for Knoevenagel condensations and transesterification reactions. *Catalysis Science & Technology* **2012**, *2* (5), 1005-1009.
40. Burgoyne, A. R.; Meijboom, R., Knoevenagel condensation reactions catalysed by metal–organic frameworks. *Catalysis letters* **2013**, *143* (6), 563-571.

41. Srirambalaji, R.; Hong, S.; Natarajan, R.; Yoon, M.; Hota, R.; Kim, Y.; Ko, Y. H.; Kim, K. Tandem catalysis with a bifunctional site-isolated Lewis acid–Brønsted base metal–organic framework, NH 2-MIL-101 (Al). *Chemical Communications* **2012**, 48 (95), 11650-11652. View Article Online  
DOI:10.1039/C2DT00433B
42. Timofeeva, M. N.; Panchenko, V. N.; Jun, J. W.; Hasan, Z.; Matrosova, M. M.; Jhung, S. H., Effects of linker substitution on catalytic properties of porous zirconium terephthalate UiO-66 in acetalization of benzaldehyde with methanol. *Applied Catalysis A: General* **2014**, 471, 91-97.
43. Zhu, L.; Liu, X.-Q.; Jiang, H.-L.; Sun, L.-B., Metal–organic frameworks for heterogeneous basic catalysis. *Chemical reviews* **2017**, 117 (12), 8129-8176.
44. Dhakshinamoorthy, A.; Heidenreich, N.; Lenzen, D.; Stock, N., Knoevenagel condensation reaction catalysed by Al-MOFs with CAU-1 and CAU-10-type structures. *CrystEngComm* **2017**, 19 (29), 4187-4193.
45. Rouhani, F.; Morsali, A., Highly effective Brønsted base/lewis acid cooperative catalysis: a new Cd metal–organic framework for the synthesis of Hantzsch 1, 4-DHPs at ambient temperature. *New Journal of Chemistry* **2017**, 41 (24), 15475-15484.
46. Rouhani, F.; Morsali, A., Fast and Selective Heavy Metal Removal by a Novel Metal-Organic Framework Designed with In-Situ Ligand Building Block Fabrication Bearing Free Nitrogen. *Chemistry–A European Journal* **2018**, 24 (21), 5529-5537.
47. Reich, B. J. E.; Justice, A. K.; Beckstead, B. T.; Reibenspies, J. H.; Miller, S. A., Cyanide-catalyzed cyclizations via aldimine coupling. *The Journal of organic chemistry* **2004**, 69 (4), 1357-1359.
48. Yang, F.-L.; Tao, J.; Huang, R.-B.; Zheng, L.-S., Temperature-Dependent in Situ Ligand Cyclization via C=C Coupling and Formation of a Spin-Crossover Iron (II) Coordination Polymer. *Inorganic chemistry* **2010**, 50 (3), 911-917.
49. Aguado, S.; Canivet, J.; Farrusseng, D., Engineering structured MOF at nano and macroscales for catalysis and separation. *Journal of Materials Chemistry* **2011**, 21 (21), 7582-7588.
50. Wang, J.-S.; Jin, F.-Z.; Ma, H.-C.; Li, X.-B.; Liu, M.-Y.; Kan, J.-L.; Chen, G.-J.; Dong, Y.-B., Au@ Cu (II)-MOF: Highly efficient bifunctional heterogeneous catalyst for successive oxidation–condensation reactions. *Inorganic chemistry* **2016**, 55 (13), 6685-6691.
51. Nguyen, L. T.; Le, K. K.; Truong, H. X.; Phan, N. T., Metal–organic frameworks for catalysis: the Knoevenagel reaction using zeolite imidazolate framework ZIF-9 as an efficient heterogeneous catalyst. *Catalysis Science & Technology* **2012**, 2 (3), 521-528.
52. Zhai, Z.-W.; Yang, S.-H.; Lv, Y.-R.; Du, C.-X.; Li, L.-K.; Zang, S.-Q., Amino functionalized Zn/Cd-metal–organic frameworks for selective CO 2 adsorption and Knoevenagel condensation reactions. *Dalton Transactions* **2019**, 48 (12), 4007-4014.
53. Das, R. K.; Aijaz, A.; Sharma, M. K.; Lama, P.; Bharadwaj, P. K., Direct crystallographic observation of catalytic reactions inside the pores of a flexible coordination polymer. *Chemistry–A European Journal* **2012**, 18 (22), 6866-6872.
54. Martínez, F.; Orcajo, G.; Briones, D.; Leo, P.; Calleja, G., Catalytic advantages of NH<sub>2</sub>-modified MIL-53 (Al) materials for Knoevenagel condensation reaction. *Microporous and Mesoporous Materials* **2017**, 246, 43-50.
55. Dong, X.; Hui, Y.; Xie, S.; Zhang, P.; Zhou, G.; Xie, Z., Schiff base supported MCM-41 catalyzed the Knoevenagel condensation in water. *RSC Advances* **2013**, 3 (10), 3222-3226.

